PCCP

PAPER

View Article Online
View Journal | View Issue

Cite this: *Phys. Chem. Chem. Phys.*, 2014, **16**, 2674

The electronegativity equalization method fused with molecular mechanics: a fluctuating charge and flexible body potential function for [Emim][Gly] ionic liquids†

Yang Wu,* Yao Li, Na Hu and Mei Hong

Received 28th September 2013,
Accepted 28th November 2013

DOI: 10.1039/c3cp54111h

www.rsc.org/pccp

Recently, experimental and theoretical studies on amino acid ionic liquid (AAIL) systems have attracted much attention. A transferable intermolecular potential approach that includes fluctuating charges and a flexible body based on a combination of the electronegativity equalization method and molecular mechanics (EEM/MM), and its application to an AAIL system containing 1-ethyl-3-methylimidazolium ($[Emim]^+$) and glycine ($[Gly]^-$) are explored and tested in this study. A consistent integration of EEM with MM requires the input of the EEM charges of all atoms into the MM intermolecular electrostatic interaction term. Compared with ionic liquid (IL) force fields, the EEM/MM model has an outstanding feature: the EEM/MM model not only presents the electrostatic interaction of atoms and their changes in response to different ambient environments but also introduces "the H-bond interaction region" in which a new parameter $k_{HB}(R_{HB})$ is used to describe the electrostatic interaction of hydrogen atoms in $[Emim]^+$ and oxygen atoms in $[Gly]^-$, which can form hydrogen bonds. The EEM/MM model gives quite accurate predictions for gas-phase state properties of $[Emim]^+$, $[Gly]^-$, and ion pairs, such as optimized geometries, dipole moments, vibrational frequencies, and cluster interaction energies. Due to its explicit description of charges and hydrogen bonds, the EEM/MM model also performs well for the liquid-phase properties of [Emim][Gly] under ambient conditions. The calculated properties, such as density, heat of vaporization, the self-diffusion coefficient, and ionic conductivity, are fairly consistent with available experimental results.

1 Introduction

Interest in room-temperature ionic liquids (RTILs) has increased tremendously owing to their properties as ideal reaction solvents, extraction solvents, electrolyte materials, and so on.[1–3] Recently, Ohno[4,5] and Kou *et al.*[6] first reported a new generation of cations and anions, which were directly derived from α-amino acids and their ester salts, and developed novel amino acid ionic liquids (AAILs). The most exciting features of these AAILs are that they have chiral centers, biodegradable characteristics, and high biocompatibility. AAILs are, therefore, ideal candidates to act as a platform for "task-specific ILs".[5,7]

Focusing on the ionic character of RTILs, one would consider the steric anisotropy of both cations and anions, as well as their differences in size and shape. Such factors make RTILs more than mere liquid salts and forces exist which counteract the strong electrostatic forces responsible for the charge ordering observed in their crystalline structures.[8] An atomistic model based on the combined molecular anisotropy of steric and electrostatic forces should give an appropriate picture of the dynamics of molecular RTILs. Indeed, most structural, thermodynamic, and transport properties of ILs are readily accessible by nonpolarizable models.[9–15] However, the picture derived thereby is still incomplete since the calculated mobility is still below that derived from experimental evidence.[16]

In 2002 Morrow and Maginn noticed a partial charge assignment by the CHELPH[17] method of a 1-butyl-3-methylimidazolium hexafluorophosphate pair in the gas phase in a noninteger molecular charge of $\pm 0.904e$.[8] Experimentally, in 1,3-dimethylimidazolium methylsulfate, a cation net charge of $0.74e$ was determined by high-resolution X-ray diffraction,[18] and the idea of a concomitant charge transfer in IL systems was born.[19,20] Although this reduction of charge implicitly includes some aspects of the polarization effects that are responsible for screening electrostatic interactions, this still poses several problems.

College of Chemistry, Key Laboratory of Green Synthesis and Preparative Chemistry of Advanced Materials, Liaoning University, Shenyang 110036, China.
E-mail: wuyoung@hotmail.com

† Electronic supplementary information (ESI) available. See DOI: 10.1039/c3cp54111h

First, the partial charges of interior atoms are not well defined. Additionally, if the electrostatic potential is reduced, the resulting charge distribution will consist of lower partial charges, and the corresponding noninteger charge of ions cannot be attributed to a charge transfer. Finally, the predicted charges are highly dependent on the conformation.[8] Combined with the broad molecular electric dipole moment distributions found by the maximally localized Wannier wavefunction method and *ab initio* calculations,[18] a more realistic model of IL systems should include accurate polarization efforts.

Polarizable empirical force fields are "effective" potentials that reflect the response of the electron density to an electrostatic field of a condensed phase environment. For IL systems, to our knowledge, polarizable force fields can be divided into two main categories: point-induced dipoles[21–27] and Drude oscillators.[28–30] The first polarizable force field was published by Yan *et al.* for [Emim][NO_3], which is based on the point-induced dipole model of Thole.[21–24] The authors found that the short-range interactions are enhanced due to the additional charge–dipole and dipole–dipole interactions, while long-range electrostatic interactions become more screened. Accordingly, the tendency towards structural inhomogeneity is enhanced. Borodin has proposed a good solution for ILs within the framework of a many-body polarizable force field.[26,27] The electronic polarization effects are incorporated *via* an isotropic atomic dipole formalism using Thole screening. In turn, the electrostatic potential around molecules is described *via* permanent charges located on atoms and off-atom sites. The undoubted success of this force field is its application beyond a few compounds of interests, and proves that ionic transport in IL systems is driven by electronic polarization effects. Another approach to include polarizability directly into a classical force field has been applied by Schrcöder and Steinhauser.[28] They used the Drude model, which mimics electric dipoles on the atoms by explicit charges on a spring rather than by point dipoles like the method of Thole. Hence, on every atom, there is a fixed charge and a further charge that is connected to the atom *via* a spring. They simulated an [Emim][CF_3SO_3] IL, and, as expected, the addition of polarization into the classical force fields dramatically affected the dynamics of the system.

In molecular dynamics simulations, another good solution to account for polarization is the use of the fluctuating charge model, which represents polarizabilities of all orders in the charge moments. Based on the electronegativity equalization method (EEM)[31,32] originally developed in the context of density functional theory (DFT),[33,34] the fluctuating charge model has been applied to many systems, such as water, microporous inorganic solids, organic molecules, dense and biomolecular systems, and so on.[35–43] Currently, a small number of fluctuating charge models for IL compounds are available. In 2008, Siehl *et al.*[44] applied the consistent charge equilibration (CQEq) method to guanidinium chloride IL systems. The QEq parameters are optimized for methyl-substituted guanidinium chlorides with only six atom types for H, C, N, and Cl to represent the atomic charges by quantum chemical calculations. The purpose of this report is to present a new empirical force field method in which the charges of all atoms are treated explicitly and are responsive to the ambient environment.

The gas-phase $[Emim]^+$ cation, $[Gly]^-$ anion, [Emim][Gly] ion pairs, and the liquid-phase [Emim][Gly] IL are chosen for the first application of the EEM/MM model, which couples fluctuating partial charges calculated by the EEM developed by Yang *et al.*[40] and molecular mechanics. The EEM/MM model improves upon previous polarizable models for IL systems in two aspects. First, the combination of EEM and molecular mechanics provides a wide ranging model that can not only evaluate the charges of all atoms and their changes in response to the ambient environment, but can also analyze the bond lengths and angles by working with nonrigid bodies which will affect the charges, and *vice versa*. Second, the special treatment of the interaction between $[Emim]^+$ cations and $[Gly]^-$ anions will enlighten our understanding of the formation and properties of the H-bond network in IL systems.

The remainder of this article is arranged as follows: Section 2 describes the EEM as well as its combination with molecular mechanics (the EEM/MM model) for the imidazolium glycine IL system. Section 3 is devoted to the details of the parameterization. Section 4 presents the results of the computation. Finally, conclusions and an outlook for future applications are given.

2 Model

2.1 EEM: electronegativity equalization method

The EEM model describes charge equilibration in molecular systems based on effective atomic charges, their electrostatic interactions, and additional local energy terms. The model is a second order expansion of the molecular energy in terms of atomic partial charges and has the following general mathematical form:

$$E = \sum_{\alpha} \left[E_{\alpha}^{*} - \mu_{\alpha}^{*} q_{\alpha} + \eta_{\alpha}^{*} {q_{\alpha}}^{2} + \frac{1}{2} \sum_{\beta \neq \alpha} \frac{q_{\alpha} q_{\beta}}{R_{\alpha\beta}} \right], \qquad (1)$$

where E_{α}^{*}, μ_{α}^{*} and η_{α}^{*} are the valence-state energy, valence-state chemical potential, and valence-state hardness of atom α, respectively; q_{α} and q_{β} are the partial charges of atoms α and β, respectively, and R is the distance between atomic sites.

The EEM formulated by Sanderson[45,46] states that when molecules are formed, the electronegativities of the constituent atoms become equal, yielding a molecular equalized electronegativity. The effective electronegativity χ of atom α can be defined using eqn (1) as the negative of the corresponding chemical potential μ, *i.e.*, the partial derivative of the total energy E with respect to the corresponding electron number or partial charges:

$$\chi_i = -\mu_i = -\left(\frac{\partial E}{\partial N_i}\right)_{R,N_j} = \left(\frac{\partial E}{\partial q_i}\right)_{R,q_j},$$

where χ_i is the corresponding electronegativity in the conceptualization of density function theory. The present study is based

on the EEM of Mortier and Yang *et al.*,[31,32,40] and we obtain eqn (2) for the effective electronegativities χ_α of atom α,

$$\chi_\alpha = \chi_\alpha^* + 2\eta_\alpha^* q_\alpha + k\sum_{\beta\neq\alpha}^{N}\frac{q_\beta}{R_{\alpha\beta}}. \quad (2)$$

Here, $\chi_\alpha^* = -\mu_\alpha^*$ are the valence-state electronegativities of atom α, and k (= 0.57) is an overall correction coefficient in the model of Yang.[40,41] The electronegativity equalization principle demands that eqn (3) applies for all atoms in the molecule,

$$\chi_\alpha = \chi_\beta = \cdots = \bar{\chi}. \quad (3)$$

This yields n simultaneous equations for an arbitrary molecule containing n atoms, which, along with the constraint equation on the molecule's net charge, can be solved to give the global molecular electronegativity $\bar{\chi}$ and the charges q_α on each atom in the molecule if all parameters in eqn (2) are known.

When extending the EEM model to a system containing many cations and anions, such as IL systems, the energy expression of eqn (1) should be modified to some degree to describe the interionic potential energy surface (IPES). Studies have shown that ILs, especially AAILs, have a strong hydrogen bonding ability that is useful for dissolving biomaterials.[4–6] When the separation distance between ions becomes small, the electron clouds begin to deform, *i.e.*, the interaction between the proton acceptor and donor has an observable effect on each other. As this interaction becomes relatively strong, a suitable spatial arrangement develops where hydrogen bonds form between cations and anions. The conformation region from the interionic arrangement where the electron clouds of the proton acceptor and the proton donor have a clear effect on each other to the spatial arrangement that causes formation of H-bonds is termed the "H-bond interaction region" (HBIR). In order to effectively describe the intermolecular H-bond interactions in the HBIR for IL systems, we introduce a new parameter $k_{HB}(R_{HB})$ extracted from the coefficient k of eqn (2). The distinction between k and $k_{HB}(R_{HB})$ is that the former is an overall optimized correction coefficient and the latter is dependent on the distance between the proton acceptor and the donor. Thus, the total energy expression of the EEM is rewritten for the IL system as eqn (4):

$$\begin{aligned} E = &\sum_{i=1}^{N_{cation}}\left\{\sum_\alpha\left[E_{i\alpha}^* - \mu_{i\alpha}^* q_{i\alpha} + \eta_{i\alpha}^* {q_{i\alpha}}^2 + \frac{1}{2}k\sum_{\beta\neq\alpha}\frac{q_{i\alpha}q_{i\beta}}{R_{i\alpha,i\beta}}\right]\right\} \\ &+\sum_{i=1}^{N_{anion}}\left\{\sum_\alpha\left[E_{i\alpha}^* - \mu_{i\alpha}^* q_{i\alpha} + \eta_{i\alpha}^* {q_{i\alpha}}^2 + \frac{1}{2}k\sum_{\beta\neq\alpha}\frac{q_{i\alpha}q_{i\beta}}{R_{i\alpha,i\beta}}\right]\right\} \\ &+\sum_{i=1}^{N}\sum_{j=1(\neq i)}^{N}\left\{\sum_{A\in i}\sum_{D\in j}{}_{(A,D\text{ in HBIR})} k_{HB}(R_{HB})\frac{q_{iA}q_{jD}}{R_{iA,jD}} + \frac{1}{2}k\sum_\alpha\sum_\beta\frac{q_{i\alpha}q_{j\beta}}{R_{i\alpha,j\beta}}\right\}, \end{aligned} \quad (4)$$

where N_{cation} and N_{anion} represent the number of cations and anions, respectively, in the IL system, and N is the summation of the number of cations and anions (*e.g.*, for a 1 : 1 IL, $N_{cation} = N_{anion}$, and $N = 2N_{cation}$). The variables $\mu_{i\alpha}^*$, $\eta_{i\alpha}^*$, and $q_{i\alpha}$ are the valence-state chemical potential, hardness, and partial charges of atom α of ion i, respectively. Upon inspection, the first two terms in eqn (4) represent the intraionic energy of cations or anions, while the third term represents the interionic interaction energy between ions. The parameter k is the same for all terms and $k_{HB}(R_{HB})$ is related to the separation distance between the proton acceptors (A) of ion i and donors (D) of ion j in the HBIR. Based on eqn (4), the effective electronegativity of atom α,

$$\begin{aligned} \chi_{i\alpha} = &\chi_{i\alpha}^* + 2\eta_{i\alpha}^* q_{i\alpha} + k\sum_{\beta\neq\alpha}\frac{q_{i\beta}}{R_{i\alpha,i\beta}} \\ &+\sum_{j\neq i}\left[\sum_{\substack{A=\alpha,D=\beta \\ A,D\text{ in HBIR}}} k_{HB}(R_{HB})\frac{q_{jD}}{R_{iA,jD}} + k\sum_\beta\frac{q_{j\beta}}{R_{i\alpha,j\beta}}\right], \end{aligned} \quad (5)$$

in which $\chi_{i\alpha}^* = -\mu_{i\alpha}^*$, is the valence-state electronegativities of atom α.

For many molecular or ionic systems, the charges also are not independent variables since there is a charge conservation constraint. For IL systems of no net charge, the constraint can be of three types: (i) the entire system is constrained to be neutral; (ii) each ion pair is constrained to be neutral; (iii) each cation or anion is constrained to be +1 or −1. Due to the reduced charge transfer observed for IL systems by experiments and theories, only the second case is used in this study. Considering that the center-of-mass of cations and anions of IL systems is usually used to calculate the microstructure, ionic translation, and dipole moment,[23,30] we calculated the center-of-mass separations between $[Emim]^+$ and $[Gly]^-$ to choose a specific neutral ion pair. Accordingly, the ion pair with the shortest separation was considered as a neutral ion pair. Because interionic charge transfer between cations and anions is assumed in this study, $N_{ionpair}$(= N_{cation} = N_{anion} for 1 : 1 ILs) charge constraint functions are considered:

$$\sum_\alpha q_{i\alpha} = 0 \quad (i = 1, 2, \ldots, N_{ionpair}). \quad (6a)$$

Accordingly, the chemical potentials of atoms will only be equal within an ion pair:

$$\chi_{i\alpha} = \chi_{i\beta} = \cdots = \bar{\chi}_i, \quad (6b)$$

for i = 1, 2,. . ., $N_{ionpair}$.

2.2 Combination of the EEM and MM for an [Emim][Gly] IL

Generally, force fields used in MM calculations describe the potential energy E of the IL system written as follows:

$$E = \sum_{bonds} E_b + \sum_{angles} E_\theta + \sum_{dihedrals} E_\chi + \sum_{nonbonded}(E_{vdw} + E_{elec}) \quad (7)$$

where the first three terms represent intermolecular bonded interactions arising from bonds, angles, and torsions. The nonbonded interactions are described in the final term of eqn (7), which include the van der Waals (vdW) and coulombic interactions of atom-centered point charges. For the moment, cross-terms, like stretch-bend coupling, *etc.* are omitted in eqn (7).

Implementation of the EEM in MM requires a combination of eqn (4) and (7). From inspection of both equations, we can

easily find that the simplest and most consistent implementation is to calculate the intermolecular electrostatic interaction E_{elec} of eqn (7) by using the EEM charges. Thus, we can obtain the energy expression of the fused EEM/MM model as,

$$\begin{aligned} E &= \sum_{\text{bonds}} K_r(r-r_0)^2 + \sum_{\text{angles}} K_\theta(\theta-\theta_0)^2 \\ &+ \sum_{\text{dihedrals}} \frac{K_\chi}{2}[1+\cos(n\chi-\delta)] \\ &+ \sum_{i}^{N}\left\{\sum_{\alpha}\sum_{\beta} 4\varepsilon_{i\alpha,i\beta}\left[\left(\frac{\sigma_{i\alpha,i\beta}}{R_{i\alpha,i\beta}}\right)^{12}-\left(\frac{\sigma_{i\alpha,i\beta}}{R_{i\alpha,i\beta}}\right)^{6}\right]\right. \\ &\left. + \frac{1}{2}k\sum_{\alpha}\sum_{\beta}\frac{q_{i\alpha}q_{i\beta}}{R_{i\alpha,i\beta}}\right\} \\ &+ \sum_{i=1}^{N}\sum_{j=1(\neq i)}^{N}\left\{\sum_{\alpha}\sum_{\beta} 4\varepsilon_{i\alpha,j\beta}\left[\left(\frac{\sigma_{i\alpha,j\beta}}{R_{i\alpha,j\beta}}\right)^{12}-\left(\frac{\sigma_{i\alpha,j\beta}}{R_{i\alpha,j\beta}}\right)^{6}\right]\right. \\ &\left. + \underbrace{\sum_{A\in i}\sum_{D\in j}}_{\text{(A,D in HBIR)}} k_{HB}(R_{HB})\frac{q_{iA}q_{jD}}{R_{iA,jD}} + \frac{1}{2}k\sum_{\alpha}\sum_{\beta}\frac{q_{i\alpha}q_{j\beta}}{R_{i\alpha,j\beta}}\right\}, \end{aligned} \tag{8}$$

in which the force field is based on the AMBER-type parameterization and q is the charge calculated from the EEM method. In this study, we use eqn (5) and (6) to compute the charges of all atoms and then use eqn (8) to compute the total energy of the system. Additionally, from time to time when there is a change in the relative position of the atoms in the IL system, we recalculate the charges using eqn (5) and (6) and then recalculate the total energy using eqn (8). Therefore, the combined EEM/MM model provides a new approach that allows for flexible geometry and fluctuating charge on all the atoms of an IL system.

3 Calibration of parameters

As an initial IL system potential for the combined EEM/MM model, we consider a transferable intermolecular potential for the fluctuating charge model. Although one of the primary objectives of this study is to determine the potential functions for the [Emim][Gly] IL, it is, of course, desirable to obtain parameters in such a way that they are transferable to other IL systems. For this study, we first calculate the geometries, frequencies, charge distributions, and dipole moments of $[Emim]^+$ cations and $[Gly]^-$ anions. The structures and atom type notations are shown in Scheme 1, and the interaction energies are also explored for the gas-phase ionic pairs. The calculated results are compared with available experiments and *ab initio* calculations to fit the parameters employed in eqn (5)–(8). The coefficients χ^* and η^* of the EEM are determined through a regression and least-squares optimization procedure and are listed in Table 1 including the Pauling electronegativity, where the Pauling electronegativity unit is used. Compared with previous values, the coefficients χ^* and η^* for the [Emim][Gly] system have been slightly altered mainly due to two factors: one factor is the difference between the molecular environments. IL systems are composed of ions only, while the previous coefficients are fitted to calculate single organic molecules, biological large molecules, water clusters, and so on. The other factor is that the coefficients can not only be used to reproduce the charges, but also the dipole moments and interaction energy in accord with available experimental and theoretical results.

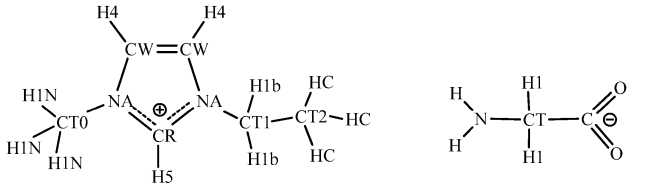

$[Emim]^+$ $[Gly]^-$

Scheme 1 Schematic structure and atom type notations of the 1-ethyl-3-methylimidazolium cation ($[Emim]^+$) and glycine anion ($[Gly]^-$) in the EEM/MM force field.

Table 1 The EEM parameters[a]

	χ^*	$2\eta^*$		χ^*	$2\eta^*$		χ^*	$2\eta^*$
CT0	2.5180	3.5204	CW	2.5400	4.6078	HC	2.2000	5.1991
CT1	2.5250	1.9050	NA	3.0430	3.2095	H4	2.1900	2.9083
CT2	2.5000	2.6716	H1N	2.1950	3.8085	H5	2.1500	1.9545
CR	2.5600	2.2856	H1b	2.2000	4.3485			
N	3.0262	3.3210	CT	2.5200	3.4522	H	2.1909	4.6940
O	3.4508	3.3320	C	2.5720	3.3602	H1	2.1809	3.3655

[a] χ^* and η^* are the parameters in eqn (2), and the Pauling electronegativity unit is used. The Pauling electronegativity scale, χ^0, for C, N, O, and H is 2.55, 3.04, 3.55, and 2.20, respectively.

The parameter $k_{HB}(R_{HB})$ is extracted from k (= 0.57) and describes the electrostatic interactions of cations and anions in the HBIR. The question arises as to the separation distance the interaction between the cations and the anions begins to enter into the HBIR and forms strong H-bond interactions. Based on previous DFT/B3LYP calculations and the molecular dynamic simulations for [Emim][Gly] by our group,[47,48] a good answer for the above question is at a separation distance of approximately 2.1 Å at which the first maximum is located from the radial distributional function (RDF) between the H atoms of $[Emim]^+$ and the O atoms of $[Gly]^-$. In addition, five configuration regions located around the carbonyl oxygen atoms of $[Gly]^-$ and the H atoms of the imidazolium ring of $[Emim]^+$ and defined as S1, S2, S3, S4, and S5 have been found to be favorable for the formation of intermolecular hydrogen bonds.[47] The corresponding $k_{HB}(R_{HB})$ of the five configurations is 0.72, 0.40, 0.73, 0.40, 0.67, 0.49, 0.50, 0.82, 0.62, and 0.47, respectively, which are used to provide the best possible relationship between the H-bond separations of the cations and anions and their interactions. And, as a result, the following expression for $k_{HB}(R_{HB})$ is used for the EEM/MM model:

$$k_{HB}(R_{HB}) = 0.7964R_{HB} - 0.9143.$$

The corresponding graph is depicted in Fig. 1. Thus, for the EEM/MM model, we assume that the electron clouds of the

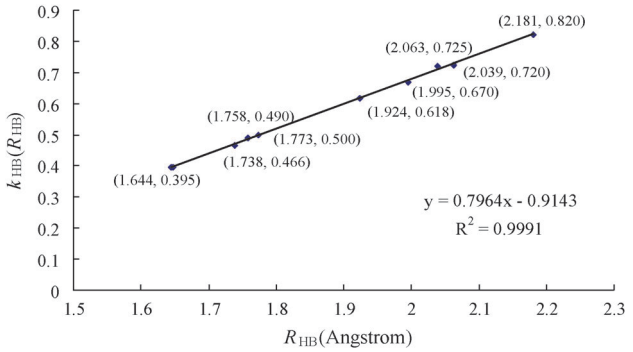

Fig. 1 Function $k_{HB}(R_{HB})$ extracted from the overall correction coefficient k (= 0.57). The function is fitted by the average distance between the O atoms of $[Gly]^-$ and H atoms of $[Emim]^+$ for the five [Emim][Gly] conformations with the corresponding k_{HB}. The fitted data are in parentheses.

H atom of the cation and the O atom of the anion would have an observable effect on each other as they approach one another to about R_{HB} = 2.1 Å. Specifically, from a separation distance of 2.1 Å, the interaction between cations and anions enters into the HBIR, and $k_{HB}(R_{HB})$ is related to the separation distance R between the H atom of the cation and the O atom of the anion. When the separation is larger than 2.1 Å, $k_{HB}(R_{HB})$ is equivalent to the overall optimized correction coefficient k.

The other parameters of the force field, K_r, K_θ, K_χ, and ε are based on the AMBER-type parametrization,[49] and this force field has been optimized specifically for imidazolium-based ILs and has been widely used in other studies.[50] A complete set of force field parameters is given in the ESI† (Table S1 and Fig. S1).

4 Results and discussion

4.1 Imidazolium cation $[Emim]^+$ and glycine anion $[Gly]^-$

Because IL systems are mainly composed of cations and anions, their correct description is essential. We first explored the optimal geometries, gas-phase charges, dipole moments, and vibration frequencies by the EEM/MM model for $[Emim]^+$ and $[Gly]^-$. The optimized structures of $[Emim]^+$ and $[Gly]^-$ from the EEM/MM model are in reasonable agreement with the *ab initio* results, as listed in Table 2. Taking $[Emim]^+$ as an example, the calculated EEM/MM model distances of H4–CW, CW═CW, and NA–CT1 are 1.074, 1.343, and 1.477 Å, respectively, and the corresponding values by DFT/B3LYP are 1.077, 1.361, and 1.484 Å using the 6-311+G(d,p) basis set. Comparison of the general EEM/MM and DFT harmonic vibrational frequencies for $[Emim]^+$ and $[Gly]^-$ is given in Fig. 2 and Table S2 (ESI†). For example, Fig. 2 shows that, for $[Gly]^-$, the linear regression equation is $y = 1.0309x - 58.138$ and the linear correlation coefficient R is 0.9958. It is clear that the frequencies from our model are slightly different from the DFT values, which is due to the fact that the EEM/MM model simulation calculations should add some additional terms, such as Euler's function, which will improve the frequency computations to some extent.

The gas-phase charges and dipole moments for the isolated cation and anion derived from the EEM/MM model are listed in Table 3. Compared to other potentials, the EEM/MM model fully considers conformational changes and molecular vibrations and provides the explicitly quantitative charges of all atoms. The positive charges located on the H atoms in $[Emim]^+$ are balanced by the negative charges on the N and C atoms. For example, as shown in Table 3, the H5 and H4 charges from the EEM/MM model are 0.2597 and 0.2633*e* (0.2725*e*) in the imidazolium ring, respectively, and the corresponding DFT/B3LYP charges are 0.2410 and 0.2508*e* (0.2503*e*). For $[Gly]^-$, the charges of carboxyl O atoms are −0.7946 and −0.8037*e*, which is also in good agreement with DFT results, −0.7933 and −0.8070*e* by B3LYP/6-311+G(d,p). As expected, the EEM/MM model reproduces the dipole moment fairly well due to the use of consistent charges. The calculated values for $[Emim]^+$ and $[Gly]^-$ are 1.570 and 4.105 Debye, and the corresponding DFT/B3LYP values are 1.656 and 4.556 Debye, respectively.

4.2 The gas-phase properties of [Emim][Gly] conformations

Dupont suggested that the pure ILs based on the imidazolium cation are H-bonded polymeric supramolecules. As mentioned

Table 2 Comparison of the EEM/MM and the B3LYP/6-311+G(d,p) derived geometrical parameters (selected) for gas-phase $[Emim]^+$ and $[Gly]^-$ (Distances are in angstroms, and all angles are in degrees)[a]

	EEM/MM	B3LYP		EEM/MM	B3LYP
CW═CW	1.343	1.361	CW–NA	1.386	1.382
CR–NA	1.337	1.336	H5–CR	1.074	1.077
H4–CW	1.074	1.077	NA–CT0	1.488	1.471
CT0–H1N	1.083	1.090	NA–CT1	1.477	1.484
CT1–CT2	1.542	1.525	CT1–H1b	1.089	1.091
CT2–HC	1.095	1.092	H5–CR–NA	125.83	125.47
CT0–NA–CW	124.93	125.72	CT1–NA–CR	126.75	125.75
CT2–CT1–NA	110.19	112.43	H4–CW–NA	123.05	122.15
H1N–CT0–NA–CW	60.76	60.19	CT2–CT1–NA–CW	79.34	73.71
H5–CR–NA–CW	179.60	180.16			
C═O	1.241	1.258	CT–C	1.565	1.567
N–CT	1.488	1.478	CT–H1	1.079	1.094
N–H	1.007	1.023	O═C═O	129.57	129.17
O═C–CT	114.95	115.61	C–CT–H1	105.38	106.79
N–CT–H1	109.82	110.07	H–N–CT	102.35	103.99
H–N–CT–H1	167.66	150.80	O═C–CT–H1	84.27	108.25

[a] The atom labels refer to those used in Scheme 1.

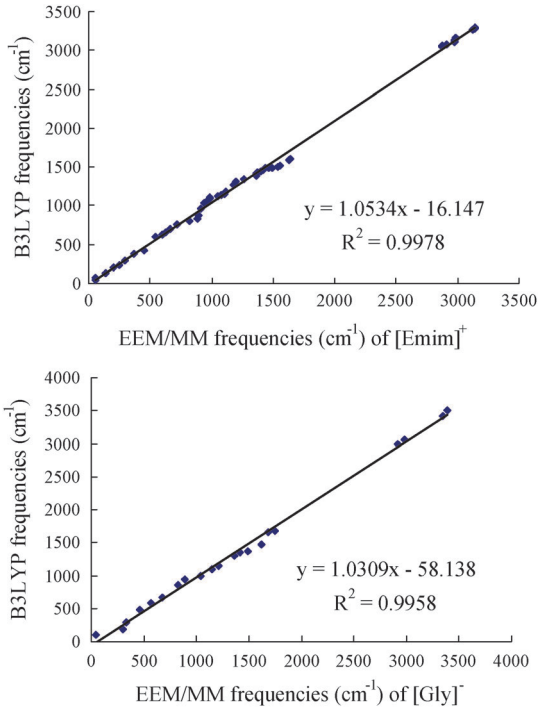

Fig. 2 EEM/MM model derived harmonic vibrational frequencies *vs.* the corresponding B3LYP/6-311+G(d,p) frequencies (cm^{-1}) of gas-phase $[Emim]^+$ and $[Gly]^-$.

above, the five regions defined as S1, S2, S3, S4 and S5 are favorable for the formation of intermolecular H bonds.[47] Fig. 3 presents the interaction patterns between $[Emim]^+$ and $[Gly]^-$ optimized using the EEM/MM model, in which we clearly considered the intermolecular H bonds expressed as $k_{HB}(R_{HB})$. The interaction energy data derived from DFT/B3LYP and the EEM/MM model are listed in Table 4. Similarly to the DFT/B3LYP calculations, our EEM/MM model also produced two short H-bond interactions in all conformers and the carbonyl O atoms of $[Gly]^-$ prefer to remain coplanar with the imidazolium ring. The [Emim][Gly]_S1 ion pair has the shortest H bond to the most acidic H5 site, which leads to the most stable isomer. The [Emim][Gly]_S2 complex also form the H5$\cdots$$[Gly]^-$ interaction though it is slightly less stable than the [Emim][Gly]_S1 ion pair (Table 4). Additionally, although the $[Gly]^-$ anion can form a H-bond with hydrogen atoms in the S3, S4, and S5 regions of $[Emim]^+$, the corresponding separation distances of those H-bonds are much longer and the interaction energies are less than those of the S1 and S2 regions. Compared with DFT/B3LYP calculations, the H-bond distances derived from the EEM/MM model are wholly larger, and the interaction energies seem to be smaller, which is partially due to the consideration of reduced charges for IL systems and will be explored in the following part.

It is interesting to calculate the harmonic vibrational frequencies for [Emim][Gly] isomers, and the comparisons of these values obtained through the EEM/MM model and DFT/B3LYP are shown in Fig. 4. The EEM/MM model gives normal modes with mostly smaller components in magnitude at high frequencies. However, it is significant that the EEM/MM model can reasonably reproduce the intermolecular mode vibrational frequencies of 2868.5, 2869.0, 2867.9, 2868.0, and 2869.2 cm^{-1} for the S1–S5 complexes, compared to the corresponding DFT values of 2473.7, 2484.8, 2754.6, 2783.1, and 2689.5 cm^{-1}, respectively. The intermolecular normal modes are undoubtedly affected by the charges.

The charges of the [Emim][Gly] isomers derived from the EEM/MM model are listed in Table 4, from which we can determine that (1) the charges for the five isomers are different in comparison with isolated $[Emim]^+$ and $[Gly]^-$ for all atoms, which is a consequence of environmental changes around the cations and anions. For an isolated cation or anion, there is no other atom or molecule to affect its electron cloud, but for an ionic pair, the formation of an intermolecular H bond will affect the electron clouds of each. The more significant changes of the five ionic pairs take place in the H atoms belonging to the $[Emim]^+$ cation and the carbonyl O atoms belonging to the $[Gly]^-$ anion. Taking the [Emim][Gly]_S2 ion pair as an example, the EEM/MM model charges for the H5 and O(=C) sites are 0.3979 and −0.8589*e*, respectively, while the corresponding values for the isolated cation or anion are 0.2597 and −0.7946*e*, respectively. (2) Although there are also some discrepancies between the calculated charges by the EEM/MM and DFT/B3LYP models, the EEM/MM model provides a much better reproduction of the charge distributions, as listed in

Table 3 Comparison of the EEM/MM and B3LYP/6-311+G(d,p) derived atomic charges (*e*) and dipole moments (Debye) for gas-phase $[Emim]^+$ and $[Gly]^-$ [a]

	EEM	B3LYP		EEM	B3LYP		EEM	B3LYP
NA	−0.3501	−0.3508	H1b	0.2178	0.2242	H4	0.2633	0.2508
CT0	−0.3585	−0.3565	NA	−0.3741	−0.3489	H4	0.2725	0.2503
H1N	0.2547	0.2303	CR	0.2389	0.2941	CT2	−0.5931	−0.5915
H1N	0.2281	0.2255	CW	−0.0258	−0.0075	HC	0.2452	0.2369
H1N	0.2541	0.2302	CW	−0.0280	−0.0054	HC	0.2451	0.2147
CT1	−0.1977	−0.1711	H5	0.2597	0.2410	HC	0.2495	0.2155
H1b	0.1983	0.2183						
Dipole	1.570	1.656						
CT	−0.1445	−0.2963	H1	0.1177	0.1708	N	−0.8717	−0.8845
C	0.7343	0.7440	O	−0.7946	−0.8070	H	0.2992	0.3246
H1	1.1060	0.1726	O	−0.8037	−0.7933	H	0.3572	0.3673
Dipole	4.105	4.556						

[a] The atom labels refer to those used in Scheme 1.

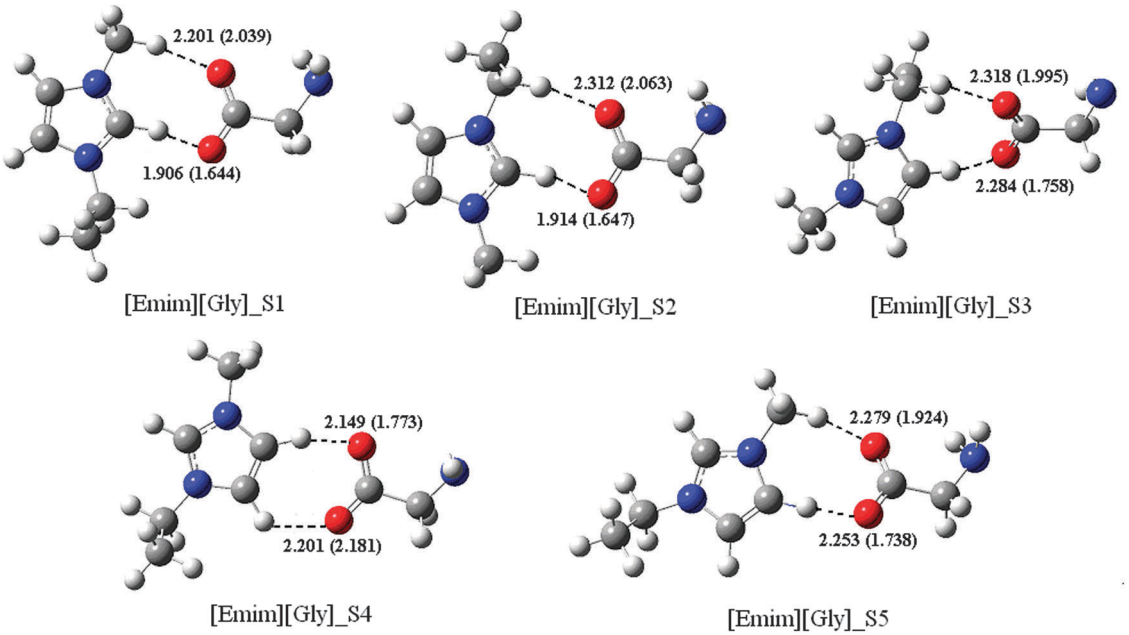

Fig. 3 Optimized conformers of [Emim][Gly], and key cation–anion distances calculated by the EEM/MM model and by B3LYP/6-311+G(d,p) (in parentheses). All distances are in angstroms.

Table 4 Comparison of the EEM/MM and B3LYP/6-311+G(d,p) atomic charges (*e*) and intermolecular energies (kJ mol^{-1}) for gas-phase [Emim][Gly] ion pairs[a]

	S1		S2		S3		S4		S5	
Charge	EEM	B3LYP	EEM	B3LYP	EEM	B3LYP	EEM	B3LYP	EEM	B3LYP
NA	−0.3558	−0.3783	−0.3998	−0.3998	−0.3406	−0.3416	−0.3048	−0.3616	−0.3219	−0.3669
CT0	−0.5201	−0.3817	−0.2832	−0.3596	−0.2341	−0.3516	−0.2535	−0.3495	−0.4374	−0.3870
H1N	0.2238	0.1993	0.1658	0.2058	0.1436	0.2162	0.1564	0.2228	0.4208	0.3012
H1N	0.4954	0.2915	0.2059	0.2526	0.1171	0.2125	0.1210	0.2028	0.1878	0.1926
H1N	0.2245	0.1995	0.1656	0.2054	0.1415	0.2147	0.1577	0.2236	0.2138	0.2050
CT1	−0.2006	−0.1768	−0.0631	−0.2013	−0.0927	−0.2011	−0.1976	−0.1680	−0.2131	−0.1694
H1b	0.2001	0.2461	0.3189	0.2900	0.1032	0.1851	0.1375	0.2018	0.1485	0.2073
H1b	0.1663	0.2005	0.1148	0.1944	0.3158	0.2959	0.1351	0.2168	0.1668	0.2130
CT2	−0.5722	−0.5857	−0.7693	−0.5842	−0.7435	−0.5928	−0.6071	−0.5873	−0.5689	−0.5863
HC	0.1948	0.1975	0.2367	0.2195	0.2323	0.2167	0.1828	0.2117	0.1948	0.2120
HC	0.2097	0.2171	0.2449	0.1910	0.2727	0.2375	0.2008	0.2061	0.1951	0.2092
NA	−0.3615	−0.3624	−0.3889	−0.3727	−0.3700	−0.3664	−0.3527	−0.3564	−0.3246	−0.3408
CR	0.2143	0.2948	0.2029	0.2952	0.1057	0.2640	0.0979	0.2426	0.1165	0.2607
CW	−0.0067	−0.0331	−0.0020	−0.0409	0.0016	−0.0507	−0.0307	−0.0176	−0.0414	0.0001
CW	−0.0085	−0.0392	0.0008	−0.0311	−0.0534	0.0015	−0.2533	−0.0250	−0.0103	−0.0512
H5	0.3531	0.3076	0.3979	0.3075	0.2619	0.2206	0.2411	0.2172	0.2315	0.2200
H4	0.1301	0.2283	0.1341	0.2275	0.1478	0.2303	0.3630	0.3146	0.3450	0.3166
H4	0.1457	0.2274	0.1475	0.2286	0.3909	0.3150	0.7668	0.2890	0.1719	0.2301
HC	0.1857	0.2180	0.2576	0.2128	0.2423	0.1889	0.1850	0.2166	0.1795	0.2179
N	−0.8259	−0.8447	−0.8269	−0.8445	−0.8277	−0.8492	−0.8295	−0.8504	−0.8254	−0.8486
CT	−0.2774	−0.2830	−0.2766	−0.2829	−0.2735	−0.2846	−0.2705	−0.2840	−0.2786	−0.2846
H	0.3914	0.3552	0.3690	0.3411	0.3636	0.3380	0.4001	0.3572	0.3991	0.3570
H	0.3657	0.3412	0.3944	0.3548	0.4007	0.3579	0.3630	0.3372	0.3630	0.3383
C	0.7854	0.7720	0.7751	0.7713	0.7631	0.7627	0.7941	0.7637	0.7727	0.7670
H1	0.2651	0.1927	0.2643	0.1947	0.2602	0.1934	0.2566	0.1883	0.2700	0.1897
H1	0.2624	0.1948	0.2669	0.1931	0.2659	0.1894	0.2510	0.1908	0.2635	0.1936
O	−0.8471	−0.8084	−0.8589	−0.8090	−0.8245	−0.8035	−0.8923	−0.8047	−0.8158	−0.7946
O	−0.8375	−0.7903	−0.7945	−0.7903	−0.7700	−0.7988	−0.8178	−0.8078	−0.8027	−0.8020
Energy	−327.92	−366.45	−303.02	−336.34	−90.05	−160.23	−245.77	−193.61	−66.20	−111.44

[a] The atom labels refer to those used in Scheme 1.

Table 4, and the linear correlation features are provided in the ESI† (Fig. S2). For the EEM/MM model, interionic charge transfer is allowed and the computational values are 0.22, 0.31, 0.36, 0.44, and 0.35*e* for the five S1–S5 isomers, respectively. These results are not

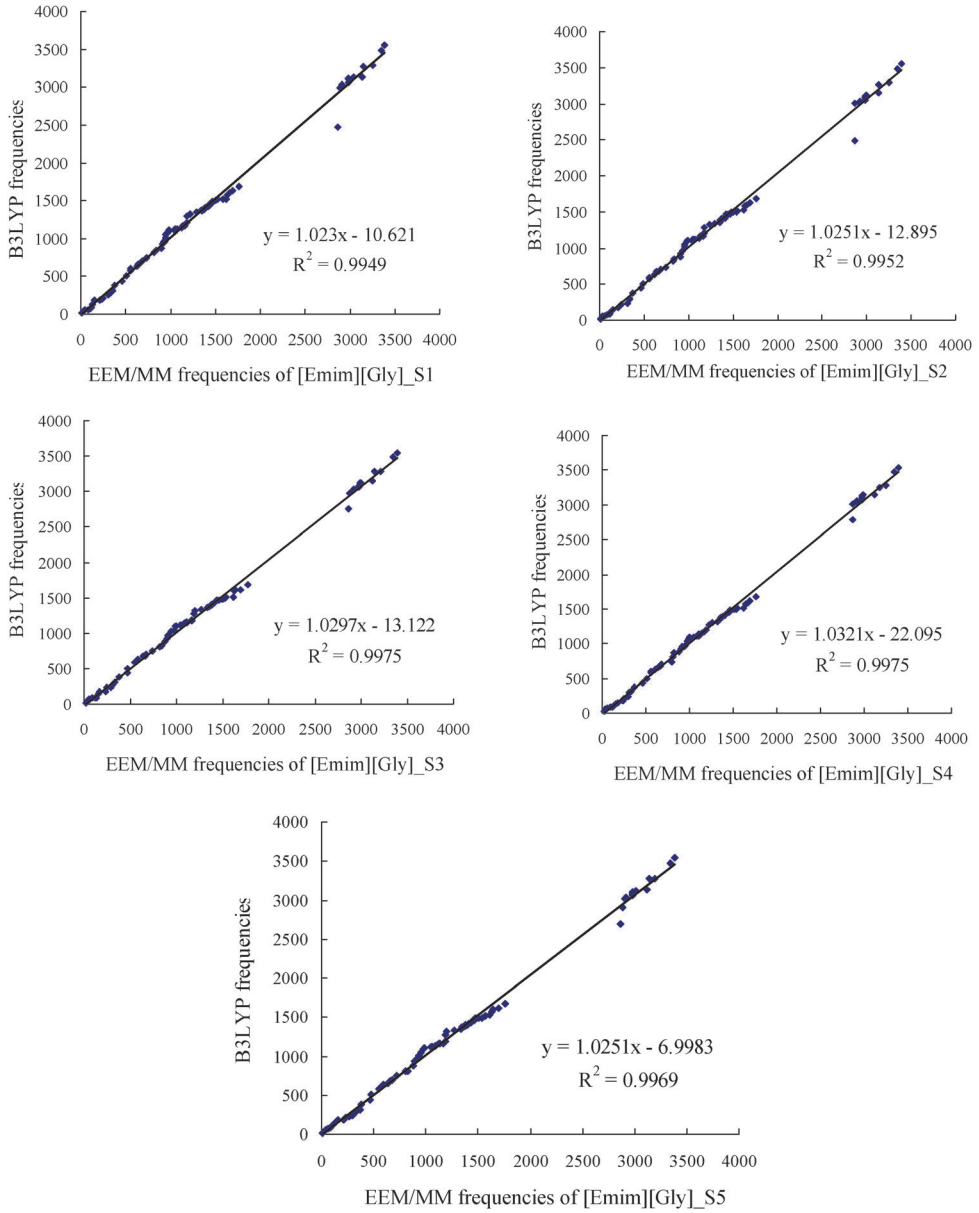

Fig. 4 EEM/MM model harmonic vibrational frequencies *vs.* the corresponding B3LYP/6-311+G(d,p) frequencies (cm^{-1}) of [Emim][Gly] conformers.

in accordance with DFT/B3LYP calculation (representing about 0.12*e* of charge transfer), but are, however, in agreement with the reduced (or scaled) charge model.[8,18,20] *Ab initio* simulations of larger aggregates and bulk liquids indicated that ion charges are between 0.6 and 0.9*e*, which provide independent justification for the use of reduced charge.[20]

4.3 Molecular dynamic simulations of liquid-phase [Emim][Gly] based on the EEM/MM model

4.3.1 Simulation details and charge distributions. All molecular dynamics (MD) simulations are performed using a modified Tinker 4.2 molecular modeling package. As mentioned above, the K_r, K_θ, K_χ, and ε parameters are based on the AMBER-type parametrization (Table S1, ESI†), and the explicit charges of all atoms are calculated by the EEM. Initial system geometries were generated by randomly inserting 192 [Emim][Gly] into the simulation cell and then allowing the system to relax for 3 ns using the fixed charge model (RESP charges) with an NVT ensemble.[48] This was followed using the EEM/MM model to equilibrate the system for 1 ns within a NPT ensemble at 298 K and 0.1 Mpa, which was controlled by the Berendsen method.[51] Finally, due to the specific viscosity of the IL system, the production stage was continued for 3 ns using an NVT ensemble with the EEM/MM model. During the production stage, configurations of the simulation box were recorded every 1 ps for subsequent structural analysis. Cubic periodic boundary conditions were used to simulate the bulk liquid, and long-range electrostatic interactions were computed using the Ewald summation. Additionally, it should be noted that rather than solving for the charges exactly at each time step, we recalculate

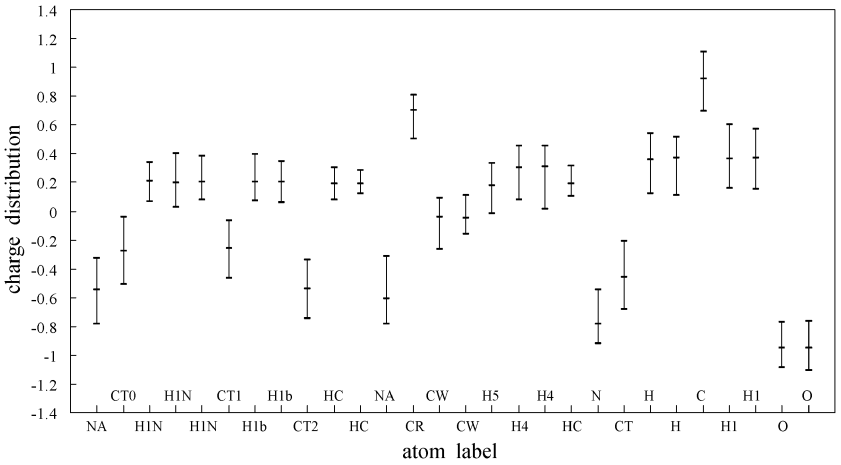

Fig. 5 Distributions of atomic charges (*e*) for liquid-phase [Emim][Gly] at 300 K as determined by the EEM/MM model. The atom labels refer to those used in Scheme 1.

the charges of all atoms every 10 ps, in the interest of economizing computational time.

The charge distributions of atoms in the liquid [Emim][Gly] derived from the EEM/MM model are shown in Fig. 5. Compared to other potentials, the EEM/MM model fully considers conformational changes and molecular vibrations and can explicitly provide quantitative charges for all atoms. For example, the computed maximum, minimum, and average charge for NA in the imidazolium ring is −0.3291, −0.7855, and −0.5464*e*, respectively; for the H5 site of $[Emim]^+$, the corresponding values are 0.3320, −0.0168, and 0.1804*e*, respectively; and for one carbonyl O atom of $[Gly]^-$, the corresponding values are −0.7685, −1.0903, and −0.9492*e*, respectively. In comparison with the charges of ionic pairs of gas-phase [Emim][Gly], two points must be mentioned:

(1) There are some discrepancies in atomic charges because of the different environments around cations and anions. Taking the N atom of $[Gly]^-$ as an example, the charge in the S1–S5 gas-phase conformations is −0.8259, −0.8269, −0.8277, −0.8295, and −0.8254*e*, respectively, whereas, in liquid [Emim][Gly], at room temperature, the average charge of the corresponding N atom is −0.7831*e*. Therefore, the more sophisticated charge model is essential to improve modeling of IL systems for all types of environments, especially for some heterogeneous solutions.

(2) Similar to gas-phase ionic pairs of [Emim][Gly], it is interesting that we can observe charge transfer between cations and anions in the liquid phase. The computed average charge transfer is 0.24*e*, which shows fair agreement with *ab initio* molecular dynamics (AIMD) simulations. Although AIMD can serve as a standard for other simulation techniques, its simulations are very computationally expensive and, currently, can only probe very small systems over a very short times.[52] Our EEM/MM model can undoubtedly reveal the importance of the polarization effect. Furthermore, the model may be used to provide uniformly scaled parameters for reduced partial charge models.

4.3.2 Thermodynamic properties. From constant-pressure MD simulations, the density, ρ, and the molar volume, V_m, of the liquid [Emim][Gly], are calculated from the EEM/MM model, as listed in Table 5. The EEM/MM model provided a value for ρ and V_m of 1.223 g cm^{-3} and 151.46 cm^3 mol^{-1} at 300 K, respectively, which is in excellent agreement with the experimental density, 1.159 g cm^{-3}, and molar volume, 159.71 cm^3 mol^{-1}, by the standard addition method at 298.15 K.[53] Compared to the fixed charge MD results (1.1960 g cm^{-3} and 154.88 cm^3 mol^{-1}),[48] the polarizable EEM/MM model has more short-range electrostatic interactions and presents a relatively large density.

The enthalpy of vaporization, ΔH_{vap}, the cohesion energy density of the particles in the liquid phase, c, and the solubility parameters, δ_H, of the IL system are related to the change in the internal energy, U_{inter}, which can be directly extracted from the simulation. Our estimations for ΔH_{vap}, c, and δ_H are calculated as

$$\Delta H_{vap} = RT - (U_{inter} - x \cdot U_{ionpair})$$

$$c = -(U_{inter} - x \cdot U_{ionpair})/V_m$$

$$\delta_H = \sqrt{c},$$

where x is the mole fraction of [Emim][Gly], R is the gas constant, and V_m is the calculated molar volume. $U_{ionpair}$ represents the intermolecular energy between the cation and anion in the gas phase, which can be obtained from DFT/B3LYP calculation (399.02 kJ mol^{-1}) in our previous work.[47] The heat of vaporization, ΔH_{vap}, for pure [Emim][Gly] is estimated to be around 141.19 kJ mol^{-1} at 300 K, which agrees well with the fixed charge model and experimentally measured values, as listed in Table 5. At 300 K, the cohesive energy density of pure [Emim][Gly] from the EEM/MM model is 915.72 J cm^{-3}, and the corresponding value is 874.37 J cm^{-3} by the fixed charge model.[48] Compared to the heavy hydrocarbons hexadecane and naphthalene,[54] the extremely high c stems mainly from electrostatic interactions, which could explain the reason that ILs have such low volatility. Additionally, the solubility parameter, δ_H, is often used to predict solubility of a solute in a solvent, which can be calculated from cohesive energy densities.[55] Despite its importance, relatively few studies have been undertaken to determine the δ_H values for ILs.[56] The calculated solubility parameter of [Emim][Gly] is 30.26 (J cm^{-3})$^{1/2}$ from the

Table 5 Density, molar volume, intermolecular energy, heat of vaporization, cohesive energy, the solubility parameter, and the ionic self-diffusion coefficient, and conductivity for the liquid-phase [Emim][Gly] IL system simulated in this work using the EEM/MM model, along with comparisons with the nonpolarizable model and available experiments

	EEM/MM	Fixed charge[a]	Experiment
ρ (g cm^{-3})	1.223	1.196	1.159[b]
V_m (cm^3)	151.46	154.88	159.71[b]
U_{inter} (kJ mol^{-1})	−542.25	−534.46	
ΔH_{vap} (kJ mol^{-1})	141.19	137.92	139.60[b]
c (J cm^{-3})	915.72	874.37	
δ_H (J cm^{-3})$^{1/2}$	30.26	29.57	
D_+ (10^{-11} m^2 s^{-1})	1.21	0.11	2.132 ($= D_+ + D_-$)[c]
D_- (10^{-11} m^2 s^{-1})	1.31	0.35	
κ (10^{-3} S cm^{-1})	6.2	1.12	4.98[c], 0.57[d]

[a] Ref. 48. [b] Ref. 53. [c] Ref. 59, and 2.132 is the sum of D_+ and D_-, which is calculated by using the Nernst–Einstein equation, on the basis of the experimental conductivity 4.98 × 10^{-3} S m^{-1}. [d] Ref. 4.

EEM/MM model. Thus, [Emim][Gly] can form aqueous biphasic systems with organic–inorganic salts, amino acids, and carbohydrates,[55] and provides real and improved (simpler, quicker, greener) alternatives to traditional extraction methods.

4.3.3 Radial distribution functions. The center-of-mass partial radial distribution functions (RDFs) of cation–anion, and site–site partial RDFs between the H5 site in the cation and the O and N sites in the anion of [Emim][Gly], for both the polarizable and nonpolarizable models, are shown in Fig. 6. A distinct feature shown in Fig. 6 is that the RDFs exhibit very long-range spatial correlations, and the oscillation extends to 18 Å, which is about the half-length of the simulation box. The effect of electronic polarization on the structure can be seen by comparing the polarizable model with the nonpolarizable model. As shown in Fig. 6, although the first maximum of $g_{+-}(r)$ has no obvious change, the relatively high second peak brings the ions in closer contact with each other for the polarizable EEM/MM model. Such effect can also be seen in the site–site partial RDFs of g_{H5-O}. Additionally, in Fig. 6, the H5−N RDF is different for the EEM and nonpolarizable models, especially at the short range. The reason for this difference is that the intermolecular hydrogen bond expression in EEM/MM, $k_{HB}(R_{HB})$ is explicitly parameterized by [Emim][Gly] S1–S5 ion pairs in the gas phase, and the N atoms are unlikely to form hydrogen bonds with cations. As electronic polarization is allowed, the more $g_{+-}(r)$ peaks can be observed and they are shifted to a shorter distance compared to the nonpolarizable model, which indicates that an additional screening effect is in operation to reduce the Coulombic repulsion between ions. Additionally, as suggested by Yan *et al.*,[24] although the simulations with polarizable and nonpolarizable models were both conducted at the same temperature, the effect of using a polarizable model appears similar to running the nonpolarizable model simulation at a higher temperature.

4.3.4 Ionic self-diffusion coefficient and conductivity. The dynamic properties of liquid [Emim][Gly], as determined by the EEM/MM model in MD simulations, are also listed in Table 5. The ionic self-diffusion coefficient and conductivity are very

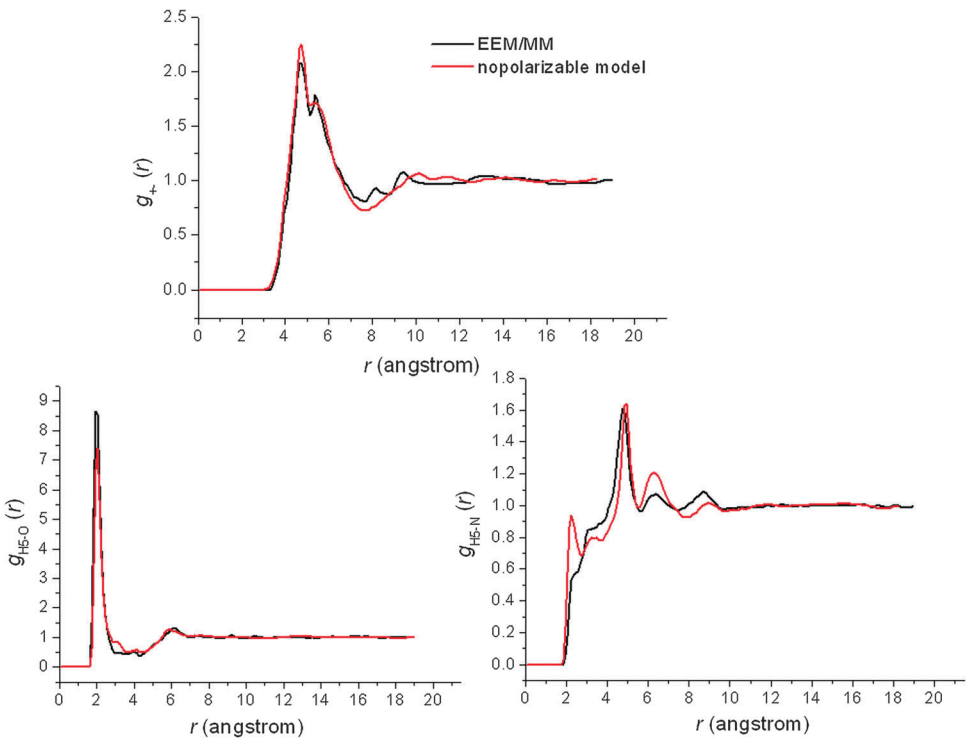

Fig. 6 Center-of-mass partial radial distributions (RDFs) for the cation−anion $g_{+-}(r)$, and site–site partial RDFs between the H5 site in the cation and O and N in the anion of [Emim][Gly], $g_{H5-O}(r)$ and $g_{H5-N}(r)$, for the polarizable EEM/MM model (black line) and the nonpolarizable mode (red line).

important parameters, due to the fact that they are time-dependent properties. The ionic self-diffusion coefficient is determined from the Einstein relation:

$$D = \lim_{t\to\infty} \frac{\left\langle |r_i(t) - r_i(0)|^2 \right\rangle}{6t},$$

where $r_i(t)$ corresponds to the position vector of the center of mass of molecule i, and the average is taken over all molecules and simulations run with an NVT ensemble. Transport properties are intimately related to short-range and long-range intermolecular potentials,[57] and provide a particularly valuable and fundamental test for a solvent model. Especially, the diffusion constant, D, is not only related to the fluctuation charge model, but also is related to the internal flexibility, although there is disagreement about whether flexibility increases and decreases the magnitude of D.[58] The values of D_+ and D_- for liquid [Emim][Gly] as determined by the flexible and fluctuating charge EEM/MM model are 1.21×10^{-11} and 1.31×10^{-11} m^2 s^{-1}, respectively, which are much similar to the experimental D_+ value of [Emim][BF_4] (4.97×10^{-11} m^2 s^{-1}).[26] Taking the strong interaction between $[Emim]^+$ and $[Gly]^-$ into consideration,[47] the relatively slow cation diffusion is reasonably compared to cationic transportation in [Emim][BF_4].

The ionic conductivity (σ) of the RTIL system can also be calculated from the self-diffusion coefficient using the Nernst–Einstein equation:

$$\sigma = N_A e^2(D_+ + D_-)/kTV_m = F^2(D_+ + D_-)/RTV_m,$$

where N_A is the Avogadro number, e is the electric charge on each ionic carrier, k is the Boltzmann constant, F is the Faraday constant, and R is the gas constant. The calculated ionic conductivity for liquid [Emim][Gly] by the polarizable EEM/MM model is 6.2×10^{-3} S cm^{-1}, which is nearly 10 times higher than Ohno's values, 5.7×10^{-4} S cm^{-1}.[4] However, this value is in good agreement with our recent experimental results (4.98×10^{-3} S cm^{-1}) from the standard addition method (SAM). We obtained a straight line when we plotted the measured conductivity against the water content in [Emim][Gly]. The intercept is the conductivity of pure [Emim][Gly].[59] Consideration of short-range H-bond interaction by $k_{HB}(R_{HB})$ in the HBIR and attenuation of long-range electrostatic interactions may be responsible for the increase of conductivity observed in comparison with the results from fixed-charge models, as listed in Table 5.

5 Conclusions

For [Emim][Gly] IL systems, we have presented a general formalism in which the transferable intermolecular potential approach includes fluctuating charges and a flexible geometry based on the EEM combined with MM. Several gas-phase properties of $[Emim]^+$, $[Gly]^-$, and [Emim][Gly] ion pairs have been first calculated by the EEM/MM model, including the optimal structure, harmonic vibrational frequency, charges, and dipole moment. The results are in fair and reasonable agreement with those measured by available experiments and *ab initio* calculations. Although the EEM/MM model underestimates high normal vibrational modes for ions, they provide a good estimate of the intermolecular mode for ion pairs. This is undoubtedly related to the consistent charge calculations, which were not included in previous IL models. Characteristic of the EEM/MM model is that the charges of [Emim][Gly] ion pairs are modified to some extent relative to an isolated cation or anion due to the different ambient environments around the monomer. The interionic charge transfers given by the EEM/MM model are relatively large for [Emim][Gly] systems, which causes the charge redistribution of the whole system and a relatively small interaction energy.

The structural and dynamic properties of the liquid [Emim][Gly] system are also studied by the EEM/MM model. The EEM/MM model quantitatively computes all atomic charges for every ion pair in the liquid [Emim][Gly] system. Especially, by introducing a specific expression $k_{HB}(R_{HB})$, the EEM/MM model explicitly explores the electrostatic interaction between donors and acceptors of hydrogen bonds, which is important to further understand the H-bonded network in AAILs. At room temperature, the EEM/MM force field gives satisfactory values for the thermodynamic properties of liquid [Emim][Gly], relative to experiments, such as density, molar volume, heat of vaporization, cohesive energy, and the solubility parameter. Furthermore, because electronic polarization is allowed, an additional screening effect is in operation to reduce the Coulombic repulsion between ions, which can be observed in the RDFs derived from the EEM/MM model. In addition, the EEM/MM model gives significantly higher ionic mobility than corresponding fixed-charged models, and performs well for the self-diffusion coefficient and ionic conductivity of liquid-phase [Emim][Gly].

Overall, the EEM/MM model shows some improvements for the liquid [Emim][Gly] system over previous IL models. The combination of the electronegativity equalization method and molecular mechanics includes not only the vibration of bond lengths and angles but also, the explicit consideration of the electrostatic interaction of all atoms (especially, the short-range interactions of hydrogen bonds), and demonstrates that it can reproduce rather accurate properties of gas and liquid [Emim][Gly]. It would be interesting to (i) extend the EEM/MM force field to make it applicable beyond a few AAILs of interest and (ii) simulate small molecules, such as water and cellobiose, in liquid AAILs. Both possibilities are being considered currently.

Acknowledgements

Calculations reported in this paper were performed on the computational clusters operated by the Computing Center, Liaoning University. The authors would like to express their gratitude to Professor Zhong-Zhi Yang at Liaoning Normal University (LNNU). We gratefully acknowledge the financial support provided by the National Natural Science Foundation of China (No. 21373104), the Natural Science Foundation of Liaoning Province (No. 20102088), the Scientific Research Foundation of the Education Department of Liaoning Province (No. L2011006), and the Foundation of 211 Project for Innovative Talents Training of Liaoning University.

References

1 R. D. Rogers and K. R. Seddon, *Science*, 2003, **302**, 792.
2 R. Hayes, S. Imberti, G. G. Warr and R. Atkin, *Angew. Chem., Int. Ed.*, 2012, **51**, 7468.
3 J. P. Hallett and T. Welton, *Chem. Rev.*, 2011, **111**, 3508.
4 K. Fukumoto, M. Yoshizawa and H. Ohno, *J. Am. Chem. Soc.*, 2005, **127**, 2398.
5 H. Ohno and K. Fukumoto, *Acc. Chem. Res.*, 2007, **40**, 1122.
6 G. H. Tao, L. He, N. Sun and Y. Kou, *Chem. Commun.*, 2005, 3562.
7 H. Peng, Y. L. Zhou, J. Liu, H. B. Zhang, C. L. Xia and X. H. Zhou, *RSC Adv.*, 2013, **3**, 6859.
8 C. Schröder, *Phys. Chem. Chem. Phys.*, 2012, **14**, 3089.
9 C. G. Hanke, S. L. Price and R. M. Lynden-Bell, *Mol. Phys.*, 2001, **99**, 801.
10 T. I. Morrow and E. J. Maginn, *J. Phys. Chem. B*, 2002, **106**, 12807.
11 S. M. Urahata and M. C. C. Ribeiro, *J. Chem. Phys.*, 2004, **120**, 1855.
12 E. J. Maginn, *Acc. Chem. Res.*, 2007, **40**, 1200.
13 B. L. Bhargava and S. Balasubramanian, *J. Chem. Phys.*, 2007, **127**, 114510.
14 C. Schröder and O. Steinhauser, *J. Chem. Phys.*, 2008, **128**, 224503.
15 T. Koller, J. Ramos, N. M. Garrido, A. P. Fröba and I. G. Economou, *Mol. Phys.*, 2012, **110**, 1115.
16 M. Salanne, L. J. A. Siqueira, A. P. Seitsonen, P. A. Madden and B. Kirchner, *Faraday Discuss.*, 2012, **154**, 171.
17 C. M. Breneman and K. B. Wiberg, *J. Comput. Chem.*, 1990, **11**, 361.
18 F. Dommert, K. Wendler, R. Berger, L. Delle Site and C. Holm, *ChemPhysChem*, 2012, **13**, 1625.
19 M. Bühl, A. Chaumont, R. Schurhammer and G. Wipff, *J. Phys. Chem. B*, 2005, **109**, 18591.
20 Y. Zhang and E. J. Maginn, *J. Phys. Chem. B*, 2012, **116**, 10036.
21 T. Y. Yan, C. J. Burnham, M. G. Del Pópolo and G. A. Voth, *J. Phys. Chem. B*, 2004, **108**, 11877.
22 W. Jiang, Y. T. Wang, T. Y. Yan and G. A. Voth, *J. Phys. Chem. C*, 2008, **112**, 1132.
23 T. Y. Yan, Y. T. Wang and C. Knox, *J. Phys. Chem. B*, 2010, **114**, 6886.
24 Y. X. Gu and T. Y. Yan, *J. Phys. Chem. A*, 2013, **117**, 219.
25 T. M. Chang and L. X. Dang, *J. Phys. Chem. A*, 2009, **113**, 2127.
26 O. Borodin, *J. Phys. Chem. B*, 2009, **113**, 11463.
27 D. Bedrov, O. Borodin, Z. Li and G. D. Smith, *J. Phys. Chem. B*, 2010, **114**, 4984.
28 C. Schröder and O. Steinhauser, *J. Chem. Phys.*, 2010, **133**, 154511.
29 C. Schröder, *J. Chem. Phys.*, 2011, **135**, 024502.
30 C. Schröder, T. Sonnleitner, R. Buchner and O. Steinhauser, *Phys. Chem. Chem. Phys.*, 2011, **13**, 12240.
31 B. G. Baekelandt, W. J. Mortie, J. L. Lievens and R. A. Schoonheydt, *J. Am. Chem. Soc.*, 1991, **113**, 6730.
32 B. G. Baekelandt, W. J. Mortie and R. A. Schoonheydt, *Struct. Bonding*, 1993, **80**, 187.
33 R. A. Donnelly and R. G. Parr, *J. Chem. Phys.*, 1978, **69**, 4431.
34 R. G. Parr and W. Yang, *Density Functional Theory of Atom and Molecules*, Oxford University Press, New York, 1989.
35 P. Bultinck, R. Vanholme, P. L. A. Popelier, F. De Proft and P. Geerlings, *J. Phys. Chem. A*, 2004, **108**, 10359.
36 T. Verstraelen, V. Van Speybroeck and M. Waroquier, *J. Chem. Phys.*, 2009, **131**, 044127.
37 T. Verstraelen, E. Pauwels, F. De Proft, V. Van Speybroeck, P. Geerlings and M. Waroquier, *J. Chem. Theory Comput.*, 2012, **8**, 661.
38 T. Verstraelen, P. W. Ayers, V. Van Speybroeck and M. Waroquier, *J. Chem. Phys.*, 2013, **138**, 074108.
39 A. Cedillo, D. Van Neck and P. Bultinck, *Theor. Chem. Acc.*, 2012, **131**, 1227.
40 Z. Z. Yang, E. Z. Shen and L. H. Wang, *THEOCHEM*, 1994, **312**, 167.
41 Z. Z. Yang, Y. Wu and D. X. Zhao, *J. Chem. Phys.*, 2004, **120**, 2541.
42 Y. Wu and Z. Z. Yang, *J. Phys. Chem. A*, 2004, **108**, 7563.
43 D. X. Zhao, L. Yu, L. D. Gong, C. Liu and Z. Z. Yang, *J. Chem. Phys.*, 2011, **134**, 194115.
44 M. Tanaka and H.-U. Siehl, *Chem. Phys. Lett.*, 2008, **457**, 263.
45 R. T. Sanderson, *Chemical Bond and Bond Energies*, Academic, New York, 1976.
46 R. T. Sanderson, *Polar Covalence*, Academic, New York, 1976.
47 Y. Wu and T. T. Zhang, *J. Phys. Chem. A*, 2009, **113**, 12995.
48 J. R. Li, *Master thesis*, Liaoning University, Shenyang, 2010.
49 W. D. Cornell, P. Cieplak, C. I. Bayly, I. R. Gould, K. M. Merz, D. M. Ferguson, D. C. Spellmeyer, T. Fox, J. W. Caldwell and P. A. Kollman, *J. Am. Chem. Soc.*, 1995, **117**, 5179.
50 M. Moreno, F. Castiglione, A. Mele, C. Pasqui and G. Raos, *J. Phys. Chem. B*, 2008, **112**, 7826.
51 H. J. C. Berendsen, D. van der Spoel and R. Van Drunen, *Comput. Phys. Commun.*, 1995, **91**, 43.
52 T. G. A. Youngs, M. G. Del Pópolo and J. Kohanoff, *J. Phys. Chem. B*, 2006, **110**, 5697.
53 J. Z. Yang, Q. G. Zhang, B. Wang and J. Tong, *J. Phys. Chem. B*, 2006, **110**, 22521.
54 J. H. Hildebrand and R. L. Scott, *Regular Solutions*, Prentice Hall, New Jersey, 1962.
55 J. H. Hildebrand and R. L. Scott, *The Solubility of Non-electrolytes*, Reinhold, New York, 3rd edn [M], 1950.
56 H. M. Luo, G. A. Baker and S. Dai, *J. Phys. Chem. B*, 2008, **112**, 10077.
57 H. J. V. Tyrell and K. M. Harris, *Diffusion in Liquids: A theoretical and experimental study*, Butterworths, London, 1984.
58 J. Anderson, J. Ullo and S. J. Yip, *J. Chem. Phys.*, 1987, **87**, 1726.
59 W. B. Duan, Master thesis , Liaoning University, Shenyang, 2013.